View metadata, citation and similar papers at core.ac.uk
brought to you by CORE
provided by CiteSeerX

4

ELECTRODEPOSITION OF GOLD

Paul A. Kohl

While all that glitters may not be gold, it is the most beautiful of all the elements in their pure form. The name *gold* comes from the Old English Anglo-Saxon word for *geolo* meaning "yellow" while the symbol, *Au*, comes from the Latin word *aurum*, meaning "glowing dawn." Historically gold was one of the first metals known. Gold has been valuable throughout the ages chiefly because of its physical properties of softness, ductility, corrosion resistance, density, and scarcity. The first gold coin dates back to about 560 BC. Gold cups and jewelry predating 3500 BC have been found in Iraq. The ancient Egyptians knew how to hammer gold into leaf as thin as 66 nm. The importance of gold as a form of currency was at a high point in the 1900s when most countries were on the gold standard. The bullion price of gold over the past 21 years is shown in Figure 4.1.

There have been about 160 metric kilotons of gold mined since it was first discovered, and it occupies about 0.005 ppm of the earth's crust. The world demand for gold in 2007 was approximately 80,000,000 troy ounces. Figure 4.2 shows the breakdown of the gold usage by industry. Jewelry comprises the largest fraction of the usage; however, much of that is not electroplated. For jewelry applications, gold is commonly alloyed with group IB or IIB metals, particularly copper, silver, platinum, and palladium, principally to improve its strength and wear resistance.

The electrodeposition of gold is a relatively new process; it has been traced to the early work of Brugnatelli in 1805 [1]. The motives behind the use of electroplated gold changed dramatically in the mid-twentieth century when the emerging electronics industry required special-purpose electrical connections. The electronics industry consumed 5,330,000 troy ounces in 1994. Figure 4.3 shows the growth in the use of gold in the electronics industry by year. The use of electroplated gold in a variety of different functions in the electronics industry has led to (1) many advances in our fundamental understanding of the electrodeposition process and (2) new electroplating technologies over the past 25 years.

Electrochemically deposited gold has satisfied many of the demands of the electronics industry. Gold has the third best electrical and thermal conductivity of all metals at room temperature. Also it has high ductility and excellent wear resistance, which are important for electrical contacts. The inertness of gold prevents the formation of insulating surface oxides (as compared to metals like aluminum). Group IIB metals (e.g., gold) are not good catalysts for other reactions, thus avoiding certain problems. For example, group IB metals (particularly platinum and palladium) can catalyze the polymerization of organic molecules forming insulating layers. In addition, gold is an excellent metal for wire bonding integrated circuits (ICs). Gold wires can be bonded to pure, soft gold pads by thermocompression bonding (300–400°C at high pressure to form a weld) or thermosonic bonding (150–200°C with ultrasonic energy to form a weld). Aluminum wires can be attached by ultrasonic bonding (ambient temperature with ultrasonic energy). These benefits have justified the high cost of gold in the packaging and interconnection of ICs.

A geographical breakdown of the use of gold in the electronics industry is also shown in Figure 4.3. Japan is the largest consumer of gold for electronic applications, followed by North America, Western Europe, and the Pacific rim (excluding Japan). Although the use of gold for electronic interconnections has maintained steady growth over the past two decades, its use has not kept pace with the more rapid growth in the microelectronics industry, primarily because of gold's high cost. The microelectronics industry has increased speed, performance, and packing density (number of transistors per unit area) while maintaining

Modern Electroplating, Fifth Edition Edited by Mordechay Schlesinger and Milan Paunovic
Copyright © 2010 John Wiley & Sons, Inc.

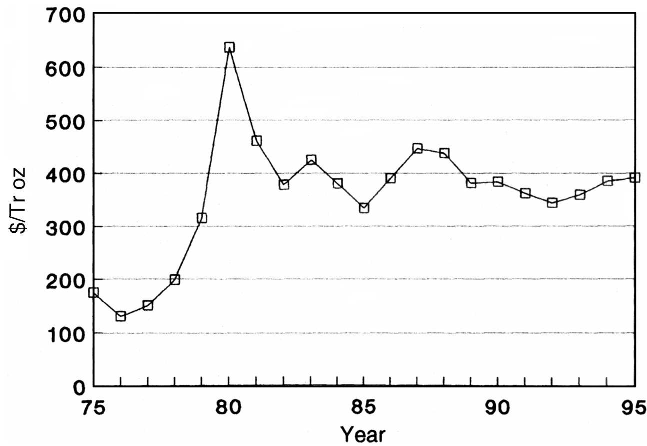

FIGURE 4.1 Gold bullion price of gold in U.S. dollars per troy ounce during the period from 1975 to 1995.

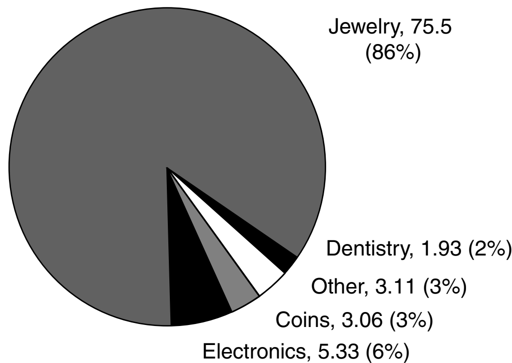

FIGURE 4.2 World gold demand in millions of troy ounces and percentage of market share by industry in 1994.

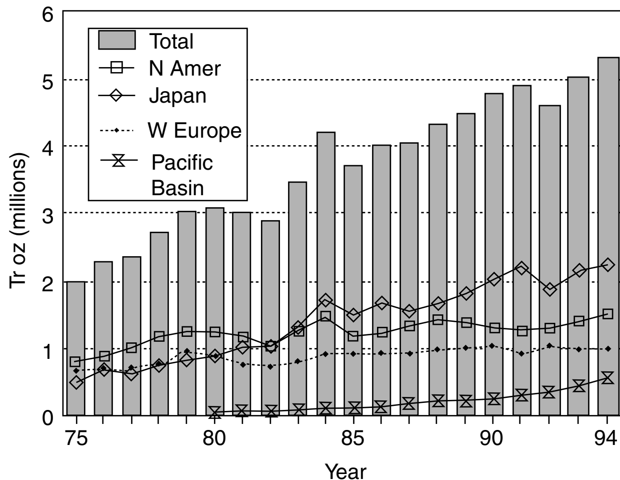

FIGURE 4.3 Gold demand in the electronics industry for Japan, North America, Western Europe, and the Pacific Basin (not Japan).

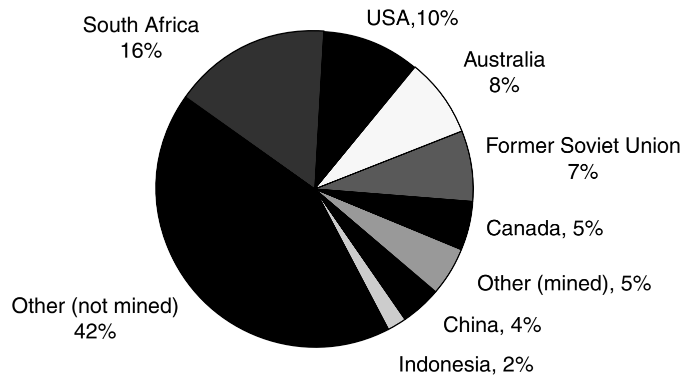

FIGURE 4.4 Gold supply in 1995 by percent. The total supply in 1995 was 98 million troy ounces.

nearly a constant cost per unit area for ICs. This has been achieved in part by reducing the consumption of expensive materials (e.g., gold), by closely controlling the amount of material needed for specific functions (thickness and area), and finding less expensive replacements for some functions. Palladium and palladium alloys have replaced gold in some electrical contact applications without a significant drop in performance.

The worldwide demand for gold has been met by recycling existing gold supplies and through the mining of metal reserves, as shown in Figure 4.4. The leading producer of mined gold is the Republic of South Africa followed by the United States and Australia.

Gold exists primarily in the $+1$ and $+3$ oxidation states. The standard potential versus the normal hydrogen electrode (NH.E) for a variety of Au(I) and Au(III) complexes is given in Table 4.1 [2, 3]. The most important ion for electrodeposition is $[Au(CN)_2]^-$. The stability of the Au(I) cyanide complex is reflected in the shift of the reduction potential for Au(I) from 1.71 V (aquo complex) to -0.611 V (cyanide complex). The stability constant for $[Au(CN)_2]^-$ is 10^{39} [4]. Two other gold complexes are of interest for electrodeposition, gold sulfite ($K = 10^{10}$) and gold thiosulfate ($K = 10^{28}$) [5]:

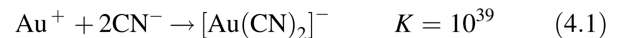

$$Au^+ + 2CN^- \rightarrow [Au(CN)_2]^- \qquad K = 10^{39} \qquad (4.1)$$

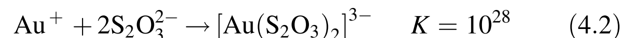

$$Au^+ + 2S_2O_3^{2-} \rightarrow [Au(S_2O_3)_2]^{3-} \qquad K = 10^{28} \qquad (4.2)$$

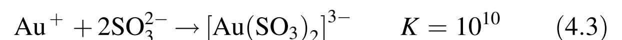

$$Au^+ + 2SO_3^{2-} \rightarrow [Au(SO_3)_2]^{3-} \qquad K = 10^{10} \qquad (4.3)$$

The potentials for the reduction of Au(III) to Au and Au(III) to Au(I), as shown in Table 4.1, are important because Au(III) can also be used as the source of gold in baths in place of Au(I), and Au(III) can also be formed at the anode during plating through the oxidation of Au(I).

In the next section, the chemical formulation of gold plating baths will be presented followed by comments on

TABLE 4.1 Standard Reduction Potentials for Gold Ions (V vs. NHE)

Half Reactions	Potential
Au(I) → Au	
$Au^{+} + e^{-} \rightarrow Au$	1.71–1.85
$AuCl_2^{-} + e^{-} \rightarrow Au + 2Cl^{-}$	1.15
$AuBr_2^{-} + e^{-} \rightarrow Au + 2Br^{-}$	0.96
$AuI_2^{-} + e^{-} \rightarrow Au + 2I^{-}$	0.58
$[Au(SCN)_2]^{-} + e^{-} \rightarrow Au + 2SCN^{-}$	0.66
$[Au(S_2O_3)_2]^{3-} + e^{-} \rightarrow Au + 2S_2O_3^{2-}$	0.15
$[Au(CN)_2]^{-} + e^{-} \rightarrow Au + 2CN^{-}$	−0.61
Au(III) → Au	
$Au^{3+} + 3e^{-} \rightarrow Au$	1.71–1.85
$AuCl_4^{-} + 3e^{-} \rightarrow Au + 4Cl^{-}$	1.0
$AuBr_4^{-} + 3e^{-} \rightarrow Au + 4Br^{-}$	0.85
$[AuI_4]^{-} + 3e^{-} \rightarrow Au + 4I^{-}$	0.56
$[Au(SCN)_4]^{-} + 3e^{-} \rightarrow Au + 4SCN^{-}$	0.64
Au(III) → Au(I)	
$Au^{3+} + 2e^{-} \rightarrow Au^{+}$	1.40
$[AuCl_4]^{-} + 2e^{-} \rightarrow [AuCl_2]^{-} + 2Cl^{-}$	0.92
$[AuBr_4]^{-} + 2e^{-} \rightarrow [AuBr_2]^{-} + 2Br^{-}$	0.80
$[AuI_4]^{-} + 2e^{-} \rightarrow [AuI_2]^{-} + 2I^{-}$	0.55
$[Au(SCN)_4]^{-} + 3e^{-} \rightarrow [Au(SCN)_2]^{-} + 2SCN^{-}$	0.62

the mechanism of gold deposition and other issues concerning the deposition process.

4.1 TYPICAL DIRECT CURRENT (DC) PLATING BATHS

Numerous proprietary gold plating baths and additives are used industrially. In this section the composition and operating parameters of representative baths are presented. The cyanide-based baths are divided into three classifications in Table 4.2: (1) the alkaline gold cyanide bath (pH > 8.5), (2) acidic, buffered baths (pH between 1.8 and 6), and (3) the neutral, buffered gold cyanide bath (pH between 6 and 8.5). The fourth group of baths, (4) noncyanide plating baths, are discussed after the three groups of cyanide baths. High-purity potassium gold cyanide, 68% metal (weight percent), can be obtained from commercial vendors in high purity.

Gold readily forms alloys with other metals during the deposition process or by diffusion with the gold substrate onto which it was plated. Gold deposits can be hard or soft, dull or bright, depending on the impurities and deposition conditions.

The potassium form of each salt is preferred over the sodium analogue because the solubility is higher. In cases where solubility is not a concern, sodium salts are sometimes used. Excessively high concentrations of gold in the baths are sometimes avoided due to the cost of the gold lost during drag-out of the salts.

The pH range between 8 and 10 is a critical region because the pK_a of hydrogen cyanide is 9.46. The equilibrium constant for HCN(aq) going to HCN(g) is $10^{1.4}$, making the pK_a for HCN(g) 8.06 [6]:

$$HCN(g) \rightarrow H^{+} + CN^{-} \qquad pK_a = 8.06 \qquad (4.4)$$

Thus, at pH > 10, the equilibrium in Eq. (4.4) is shifted to the right, and free cyanide is stable in the bath. At pH < 8, the predominate form of cyanide is HCN(g), which evolves as a gaseous product. HCN gas is highly toxic, and its evolution from plating baths is a health concern. Appropriate ventilation is required for all cyanide baths. The presence of significant concentrations of free cyanide in the bath, such as in the case of alkaline baths, is also a health risk because accidental cyanide ingestion or injection can occur.

The presence of free cyanide in the bath is a major consideration in the selection of the anode and metal ion replenishment method. In the presence of free cyanide, gold metal can be used as a consumable anode because it can be electrochemically oxidized forming the gold cyanide complex. In the absence of free cyanide, gold is not oxidized to any appreciable extent, so it acts like an inert electrode. The ramifications of this will be included for each bath.

TABLE 4.2 Typical Cyanide-Based Plating Baths (Concentrations in $g\,L^{-1}$)

Bath	Alkaline Cyanide		Buffered Citrate		Buffered Phosphate	
Operation	Rack	Barrel	Rack	Barrel	Rack	Barrel
$KAu(CN)_2$	12	6	20	20	20	20
KCN	20	30				
K_2HPO_4	20	30	—	—	40	40
KH_2PO_4					10	10
K_2CO_3	20	30	—	—		
K_2H citrate			50	50		
T (°C)	50–60	50–65	60–70	60–70	60–70	60–70
I ($mA\,cm^{-2}$)	1–5	1–5	1–2	4–6	0.7–2	4–6
pH	11–11.5	11–11.5	4–5.8[a]	4–5.8[a]	6–8	6–8

[a] pH may drift during use. Citric acid or KOH can be used to adjust pH.

4.1.1 Alkaline Cyanide Baths

Alkaline cyanide baths operate at high pH and with an excess of free cyanide. The potassium gold cyanide concentrations used in the low-current-density baths shown in Table 4.2 range from 2 to $12\,g\,L^{-1}$, with $6\,g\,L^{-1}$ often used. Higher gold concentrations will support higher current densities.

Potassium cyanide is often used as the source of the free cyanide in these baths. Since there is appreciable free cyanide present, the cyanide released during the deposition reaction does not significantly alter the cyanide concentration in the bath. Thus the Nernstian shifts in the reduction potential of Au(I) cyanide due to accumulation of free cyanide (even in the vicinity of the electrode surface) do not occur. In lower pH baths, large shifts in the free-cyanide concentration at the electrode surface have many ramifications, including a shift in the reduction potential during deposition. The excess cyanide permits the use of gold anodes for the replenishment of the metal plated from the bath:

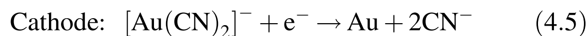

$$\text{Cathode:}\quad [Au(CN)_2]^- + e^- \rightarrow Au + 2CN^- \qquad (4.5)$$

$$\text{Anode:}\quad Au + 2CN^- \rightarrow [Au(CN)_2]^- + e^- \qquad (4.6)$$

$$\text{Full cell:}\quad \text{No change to plating solution} \qquad (4.7)$$

The main changes that occur in the bath are due to oxidation or reduction side reactions, drag-out of plating salts, and drag-in of water or impurities. The free cyanide promotes the corrosion of the gold anode (forming $[Au(CN)_2]^-$), increases the throwing power, and improves the conductivity. Free cyanide also retards the codeposition of some metals because the stability of their cyanide complexes shifts their reduction potential to values more negative than those used during deposition. The absorption of atmospheric carbon dioxide increases the concentration of carbonate in the solution as a result of the reaction between cyanide and CO_2. The carbonate can help to stabilize the pH and improve throwing power slightly.

Nonsoluble, dimensionally stable anodes, like platinized titanium or stainless steel, are sometimes used. Oxygen gas and hydrogen ions are the dominant products at the insoluble, dimensionally stable anodes, as shown in Eq. (4.9):

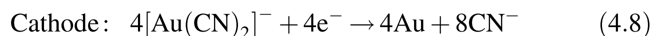

$$\text{Cathode:}\quad 4[Au(CN)_2]^- + 4e^- \rightarrow 4Au + 8CN^- \qquad (4.8)$$

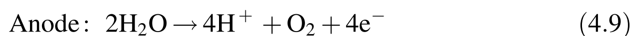

$$\text{Anode:}\quad 2H_2O \rightarrow 4H^+ + O_2 + 4e^- \qquad (4.9)$$

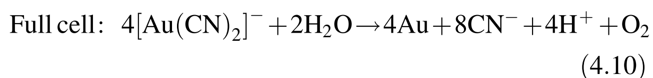

$$\text{Full cell:}\quad 4[Au(CN)_2]^- + 2H_2O \rightarrow 4Au + 8CN^- + 4H^+ + O_2 \qquad (4.10)$$

The hydrogen ions produced in Eq. (4.9) and shown in Eq. (4.10) for the full cell can either be neutralized by hydroxide (lowering the pH of the solution) or form HCN (g) and evolve from the bath as a gas depending on the operating pH, as shown previously in Eq. (4.4). Thus the pH and the gold cyanide ion concentration of the bath in Eq. (4.10) will drop as current is passed, as shown by the two half reactions. Both these effects must be reversed through the addition of plating salts and KOH. The addition of KOH and $KAu(CN)_2$ as a replenishment for the right-hand side of Eq. (4.10) will result in the accumulation of KCN (in the form of K^+ and CN^- until the KCN solubility product is reached) in the bath. The buildup of KCN is somewhat mitigated by drag-out. An insoluble anode is convenient because the cathode current distribution is reproducible and consistent over long periods of time. Also the anode docs not have to be replaced as it corrodes. Thus, anode maintenance is replaced by bath maintenance [KOH and $KAu(CN)_2$ additions].

The cathodic current efficiency for the deposition of the metal from alkaline baths can be as high as 90–100% with adequate gold content in the bath and sufficient agitation [7, 8]. For example, 100% efficiency has been obtained at $10\,mA\,cm^{-2}$ and $12\,g\,L^{-1}$ $KAu(CN)_2$ under mild agitation, whereas the current efficiency was only about 50% at $4\,g\,L^{-1}$ $KAu(CN)_2$ (otherwise similar conditions) [7].

The preferred operating temperature of the baths is 50–60°F. The codeposition of impurities (e.g., antimony) will increase the hardness and brightness of the deposits [9]. The codeposition of silver, nickel, copper, and cobalt has been used to alter the color of the deposit. This effect is used mostly for decorative purposes.

Alkaline bath formulations are generally not compatible with many polymers used in the microelectronics industry. The high-pH and high-cyanide concentration degrades photoresist and organic laminates. Thus there has been considerable work on developing neutral pH formulations. The alkaline, soft gold deposits are not acceptable for sliding electronic contacts in telephones where wear resistance is critical. The parts will gall and fail quickly.

4.1.2 Acid Cyanide Baths

The nonalkaline, cyanide-based baths which contain other metals normally use a citrate buffer and operate around pH 4. Low-pH buffered baths were originally developed for the jewelry trade but now find wide application throughout the electronics industry for contact surfaces, corrosion protection, bonding surfaces, and special electroforming. The pH of the baths allows the use of photoresist and other polymers. Typical formulations are given in Table 4.2. Anodes in these baths are usually platinized titanium, gold, or gold-plated platinized titanium. The gold-plated electrodes are found not to dissolve readily at low current densities because of the low free-cyanide concentration. This, however, is not the case at high current densities and low solution volume where

appreciable transient concentrations of free cyanide can build up and lead to the oxidation and dissolution of a pure gold anode. Stainless steel and carbon anodes are found to introduce contamination, and their use is discouraged. The use of insoluble anodes requires that plating salts be added to the bath to replenish the gold content [e.g., $KAu(CN)_2$] and maintain pH control. Although K^+ removal and pH control can be accomplished by an ion exchange method, drag-out and salt addition are the usual method of bath maintenance [10].

The codeposition of other metals with gold is easily accomplished in acid cyanide baths, resulting in marked changes in the physical properties (especially hardness) of the deposits. Hard gold is of great importance to electronic components where low contact resistance, pore-free deposits, wear resistance, and chemical inertness are functional requirements. Such applications include the multiple-insertion electrical contacts found on printed wiring board contacts or spring contacts.

Bright, hard deposits can be produced from alkaline and acid cyanide baths containing cobalt, nickel, indium, silver, arsenic, or cadmium. However, the most reliable connector finish is from acid cyanide baths with nickel or cobalt salts as the brightener [11–13]. A typical range of concentrations is given below [14]:

$KAu(CN)_2$	12–15 $g\,L^{-1}$
Citric acid	90–115 $g\,L^{-1}$
Cobalt (added as acetate or sulfate)	0.07–0.1 $g\,L^{-1}$
pH (adjust with KOH)	3.6–4.7
Temperature	40–65°C

To establish the proper pH, KOH is added to the bath. A concentration of 50 $g\,L^{-1}$ KOH will produce a bath of about pH 4.0 [14]. Baths that produce pure gold deposits often operate at close to 100% current efficiency [15]. A yellow color that develops in the bath has been attributed to the formation of the $[Co(CN)_6]^{3-}$ complex [14]. The typical grain size of cobalt-hardened gold is 225–275 Å [16].

The high current density used in high-speed baths can produce a temporary buildup of free cyanide in the bath that may lead to the corrosion of a gold anode or even the slow oxidation of a platinum anode. It has also been found that $[Au(CN)_4]^-$ can be formed at the anode, especially under high current and high cobalt concentrations at a platinum anode [17]. The buildup of Au(III) results in lower current efficiencies at the cathode for the production of gold metal because it takes 3 $eq\,mol^{-1}$ to reduce $[Au(CN)_4]^-$ to Au whereas it only takes 1 $eq\,mol^{-1}$ to reduce $[Au(CN)_2]^-$ to Au.

One of the limiting factors for the current density is the rise in pH in the vicinity of the electrode during the reduction process, through either gold deposition or hydrogen gas production. For example, at pH 3.5 and 15 $g\,L^{-1}$ $KAu(CN)_2$, the current efficiency is 20–30% for current densities less than 50 $mA\,cm^{-2}$ [13]. Hydrogen gas is the main side product of the cathodic reaction. The reduction of the gold cyanide complex is inhibited by the cobalt ion, as seen by the Tafel slopes (see Section 4.2 on deposition mechanisms), significantly dropping the current efficiently [13, 18]. The cobalt content of the pH 3.5 bath is a complex function of current density and mass transport [13]. The typical range of the incorporated cobalt is around 0.05% of the gold at high current density ($>$50 $mA\,cm^{-2}$) and low agitation [Reynolds number (Re) $<$ 3000] to 0.6% of the gold at low current (25 $mA\,cm^{-2}$) and high agitation (Re $>$ 13,000).

At higher pH or higher temperature, the cobalt and carbon contents of the deposit decrease [19]. An increase in pH above 5.5 virtually eliminates the cobalt from the deposit, which demonstrates the ability of acid cyanide baths to codeposit metals with gold. Lower current densities (smaller rate of consumption of protons at the cathode) or higher mass transport (higher rate of delivery of protons from the solution) will mitigate the rise in pH in the electrode boundary layer during deposition. Thus the higher the solution agitation, the greater is the allowable current density. The cobalt or nickel ions are known to codeposit in the gold in at least two different forms, the cyano complex and as a substitutional alloy [20–22]. The increase in hardness is due to the grain-refining effect of the codeposited cyano complex [23].

The porosity of the deposited gold also decreases with higher mass transport and lower current density [13]. The lowest porosity cobalt-hardened gold deposits were obtained at 2 $mA\,cm^{-2}$ and Re $>$ 9000.

Although cobalt salts are the most common hardening agents for acid cyanide baths, the addition of nickel acetate ($\sim$ 1 $g\,L^{-1}$ nickel) to the citrate bath also results in the hardening of the deposit and a drop in the current efficiency [12]. The wear properties of high-speed gold deposits were studied as a function of nickel or cobalt concentration, the form of the cobalt complex in solution (strongly chelating vs. weakly chelating), and current density using commercial baths [24]. The stronger chelating agent was shown to prevent the formation of cyanide complexes. Strongly chelating nickel was found to have the widest operating window. Cobalt concentrations from 1.0 to 2.0 $g\,L^{-1}$ and current densities from 100 to 500 $mA\,cm^{-2}$ were acceptable. As stated above, the weakly chelating cobalt complex required only 0.1 $g\,L^{-1}$. Most deposits showing good wear characteristics were bright; however, all bright deposits were not wear resistant. Although specific ranges for cobalt or nickel were studied, no fundamental basis for the wear properties was established. Generally speaking, empirical relationships for the bath parameters are used to optimize wear properties.

The addition of iron salts to the plating bath will harden the gold deposit, just as cobalt and nickel do. However, iron-hardened gold is much more brittle than cobalt- or nickel-hardened gold, which is unacceptable in many applications

where ductility is critical, such as in electrical contacts. The accidental contamination of baths with iron is a concern whenever iron or steel parts are used in bath construction, piping, or pretreatment equipment.

Liljestrand et al. studied the effect of nickel concentration and other plating parameters on wear for nickel-hardened gold at 60°C, $16\,g\,L^{-1}$ gold concentration, and pH 3.8–4.8 [25]. The nickel concentration in the bath was varied and the resulting content in the deposit ranged from 0.2 to 2.5 wt %. In the higher current density range from 10 to $40\,mA\,cm^{-2}$, the wear changed from severe to mild and then to brittle upon increasing the nickel content. However, in the current density range from 1 to $16\,mA\,cm^{-2}$, the wear changed from severe to adhesive brittle and then to mild with increasing nickel content. The terms *severe*, *adhesive brittle*, and *mild* refer to the physical, conditions of the surface. The severe wear at low nickel content was characterized by cold welding between the spring and pin used in the test. During the first wear cycles, the gold was smeared from one part to the other followed by early failure (less than 200 wear cycles). At high nickel content, plated at low current density, brittle wear occurred characterized by cracks reaching down to the nickel underplate. This clearly shows the need for tight control over bath and plating parameters with metal-hardened gold. X-ray diffraction was used to show an increase in the lattice contraction strain with increasing nickel content. Since the solubility of nickel in gold is about 5%, it was concluded that most of the nickel is in a solid solution and that the hardness is due to lattice strain caused by the soluted nickel atoms.

The codeposition of an insulating film from cobalt- or nickel-hardened acid gold baths has caused significant problems for electrical contacts. High electrical resistivity can be observed upon thermal aging (e.g., 150°C), especially in films plated at high speeds with high cobalt concentration [26]. The subject has received considerable attention since the late 1960s when high contact resistance on telephone spring contacts was correlated with an orange-brown film on gold-plated contacts. Munier was the first to isolate the transparent film on the cobalt-hardened gold and presumed it to be an organic polymer [27]. The indiscriminate use of the word "polymer" to refer to either the electrodeposited inclusion or the extract from the plated metal is not correct. Nevertheless, most of the literature published on the identification and elimination of the material refers to it as an insulating codeposited polymer.

Microchemical determination of the carbon content of the gold deposited from cobalt- or nickel-hardened baths based on citrate-buffered gold cyanide provides a clear link between a carbonaceous impurity and the insulating film, as shown in Table 4.3 [27]. In the absence of cobalt or nickel or at high pH (i.e., pH > 10 using a phosphate buffer and potassium gold cyanide) in the presence of cobalt salts which are not codeposited, no carbon is detected in the deposit.

TABLE 4.3 Determination of Carbon in Gold Deposits[a]

Gold Bath	Hardener	Carbon in Gold (%)
Potassium gold cyanide, $13\,g\,L^{-1}$	None	0.01–0.04
Potassium hydroxide, $15\,g\,L^{-1}$	Cobalt	0.20–0.30
Citric acid, $90\,g\,L^{-1}$	Nickel	0.19–0.43
Cobalt or nickel citrate, $0.3\,g\,L^{-1}$		

Note: pH range 3.6–4.5.

Carbon-14 labeled complexes were used to quantity the carbon content in the deposits at levels in excess of 1% [28]. Electron microscopy studies showed the deposits to exist in discrete pockets usually 1000 Å and smaller in size with a few as large as 25,000 Å [29]. A study of gold deposited from pure potassium gold cyanide as a function of temperature, of current density, and with anode isolation (in a separate compartment) led to the conclusions that (1) the carbonaceous contamination was minimized at temperatures above 65°C, (2) deposits plated at lower temperature (~ 25°C) had more carbon and were much harder and brittle, and (3) the carbon was the result of a cathodic process only and not the re-reduction of an oxidized species released from the anode [30]. However, it led the authors to the inaccurate speculation of the origin of the carbon as potassium cyanide, Au(I) cyanide, potassium cyanoaurate, or hydrogen cyanide. Mossbauer spectroscopy was later used to show that no AuCN, $KAu(CN)_2$, or $KAu(CN)_4$ were in the deposit [31].

A detailed study of the gold appearance and carbon and cobalt contents as a function of pH clearly showed the drop in codeposited cobalt and carbon as the pH was increased to 6 [19]. The slow change in the cobalt-containing hard gold solution from reddish-pink, the color of Co^{2+} citrate, to yellow, the color of $[Co(CN)_6]^{3-}$, was noted. This occurred as free cyanide was released from the reduction of $[Au(CN)_2]^-$.

A study by Okinaka et al. [14] clarified many issues. It was shown that the carbon-containing deposits obtained from dissolving cobalt-hardened gold in aqua regia were not an organic material but the cobalt complex $Co_3^{II}[Co^{III}(CN)_6]_2 \cdot xH_2O$. When dissolved in mercury, $K_3Co^{III}(CN)_6$ was found. It was concluded that there is an additional source of both cobalt and carbon in the gold deposit apart from the cobalt cyanide complex. Substitutional metallic cobalt is the additional source of cobalt.

4.1.3 Neutral Cyanide Baths

Nonalkaline baths exhibit a wider range of physical and chemical properties than possible at higher pH. In the previous section on acid baths, it was related that the codeposition of other metals from the bath provided metallurgical hardening of the deposit. The hardness is the result of a reduction in the grain size of the gold caused by the codeposit

increasing the rate of grain nucleation. It was also noted that the amount of codeposited metal (e.g., cobalt or nickel) decreased to nearly zero at $pH > 5.5$. Although the metals used to harden gold are not readily codeposited from neutral pH baths, it has been found that hard gold (as well as soft gold) can be formed in neutral baths by the careful selection of the plating parameters without the use of additives. In the neutral baths the gold salt used is the same as in alkaline and acid baths, $KAu(CN)_2$. The neutral pH and absence of free cyanide make these formulations the preferred ones for use with photoresist and other polymeric materials.

The neutral baths shown in Table 4.2 produce pure, soft gold at relatively low current densities, typically 2–5 $mA\,cm^{-2}$ and 60–70°C. The phosphate salts serve only as the supporting electrolyte and pH control, so that strict control of their concentration is not critical. The phosphate buffer can be used for acid, neutral, or basic conditions with pH adjustment carried out by the addition of KOH or H_3PO_4. Control of pH, temperature, and gold concentration is critical.

Additive-free hard gold (AFHG) can be produced from neutral baths using phosphate as the buffer, as shown in Table 4.4 [32]. Although the "low-speed" column is under acid conditions, it is included here for completeness because of its similarities with the high-speed AFHG bath. The advantages of AFHG baths over metal hardened baths are (1) no need to control additive concentration, (2) high current efficiency, (3) greater tolerance for heavy metal impurities due to the insolubility of many metal phosphates, and (4) high ductility and thermally stable contact resistance for electronic components.

However, AFHG baths are highly susceptible to bath contamination. Small amounts of impurities, such as nickel, cobalt, or iron ions, can cause large changes to the physical properties deposited from the bath. It can be difficult to purge the plating bath of the unwanted impurities.

AFGH plating was first observed in 1974 [33]. It was shown that the grain size of the deposits from the AFGH bath was 250–750 Å, which is slightly larger than those from the cobalt-hardened bath (225–275 Å) but much smaller than the grains from soft gold (1–2 μm) [16]. AuCN is codeposited in AFHG and accounts for about 50–70% of the carbon content in the deposit. The deposited AuCN forms a polymeric structure and hardens the gold by promoting the nucleation of grains or by inhibiting the growth of the existing gold grains, in a role analogous to cobalt hardening of acid gold baths mentioned in the previous section [34]. Thus the conventional bath (Table 4.2) that produces soft gold at 70°C will produce hard gold at 25°C. The population density of the AuCN in AFHG gold plated from a bath containing $KAu(CN)_2 = 44\,g\,L^{-1}$, $KH_2PO_4 = 100\,g\,L^{-1}$, $KOH = 28\,g\,L^{-1}$, and pH 7.0 was $10^{17}\,cm^{-3}$ with a volume ratio of 1.3–1.9% [34].

Data on the plating efficiency and deposit appearance of an additive-free, neutral bath is shown in Table 4.5 [32]. At low current density, the hardness was found to be independent of temperature in the range of 10–45°C ($\sim 160\,KHN_{25}$), whereas the hardness decreased to 104 KHN_{25} at 70°C. At higher plating speeds, 86–252 $mA\,cm^{-2}$ and 30–43°C, the hardness was about 180 KHN_{25}. Wear tests using lubricated sliding contacts showed severe galling for the soft gold plated at 70°C (104 KHN_{25}), whereas the harder deposits formed at lower temperatures (22–45°C) showed excellent wear. The AFHG bath was shown to have superior tensile strength, total elongation (high ductility), and more stable contact resistance than comparable deposits from a cobalt-hardened acid bath. However, a small increase in contact resistance was found when the deposit was heated to >100°C due to the surface segregation of AuCN [34].

The effect of gold cyanide concentration on current efficiency and the appearance of the finish for the high-speed bath are shown in Table 4.5 [32, 35]. The conditions were the same as the "high-speed" portion of Table 4.4 except for the gold cyanide concentration. At $KAu(CN)_2$ concentrations below 23 $g\,L^{-1}$, a matte finish was obtained with cathodic current efficiencies of 80–85%. At $KAu(CN)_2$ concentrations from 23–44 $g\,L^{-1}$, a bright finish was obtained and the current efficiency was 90–95%.

Certain metallic additives can be used as a grain refiner in the baths, such as thallium or arsenic, to increase the

TABLE 4.4 Bath Composition and Plating Conditions for Additive-Free, Neutral Gold Plating Bath

	Low Speed	High Speed
$KAu(CN)_2$	40 $g\,L^{-1}$	44–59 $g\,L^{-1}$
KH_2PO_4	100 $g\,L^{-1}$	100 $g\,L^{-1}$
pH (KOH of H_3PO_4)	4.3–4.5	6.5–7.5
Temperature	25 ± 2°C	40 ± 2°C
Agitation	Mild	Vigorous
Current density	10–20 $mA\,cm^{-2}$	200–300 $mA\,cm^{-2}$

TABLE 4.5 Appearance and Plating Efficiency of High-Speed Additive-Free Hard Gold

Temperature (°C)	Current Density ($mA\,cm^{-2}$)	Appearance	Plating Efficiency (%)	Hardness
20	121	0	78	
25	198	0	72	
25	155	2	81	
25	138	3	81	
25	121	4	86	
30	155	2	83	193
30	138	4	85	
43	259	2	87	
43	172	5	85	188
61	172	0	91	
61	86	0	82	

Note: Visual appearance defined as 0 = burned appearance to 5 = completely bright.

brightness/smoothness range of the deposit. The military specification for bondable gold (MIL-G-45204B) requires that chromium, copper, tin, lead, silver, cadmium, or zinc not be present in the deposit at a concentration greater than 0.1%.

The residual stress of gold films deposited on silicon wafers is important for microsystems and microelectromechanical systems (MEMSs). Gold is an excellent structural and contact material for MEMSs because it is difficult to oxidize. The residual stress of gold films annealed at different temperatures plated from a neutral-pH cyanide bath was measured [36]. Recrystallization of the gold occurs at high temperature, which relieves the stress due to mismatch of the coefficient of thermal expansion (CTE) between the gold and the silicon substrate. Normally, the gold achieves a stress-neutral point at the highest temperature. The CTE mismatch between the metal and the substrate caused tensile stress in the gold during cooldown. Stresses on the order of 50, 200, and 350 MPa were observed at anneal temperatures of 100, 250, and 400°C [36].

Residual stress is a particular problem for free-standing gold structures where flatness is desired, such as in X-ray lithography masks. The stress films deposited from a neutral-pH cyanide bath was found to be 50 MPa tensile whereas the addition of 25 ppm arsenic changes the stress to 30 MPa compressive. Pulsed current reduced the stress to <5 MPa compressive [37]. In other applications, the stress gradient in gold films deposited at different conditions was used to build precise-curvature cantilever beams for microswitches [38].

Anodes in these baths are normally platinized titanium, gold, or gold-plated platinized titanium. Stainless steel and carbon anodes are not recommended because of contamination. Gold or gold-plated anodes do not dissolve readily because the concentration of free cyanide is very low. However, at high current density and small solution volumes (or close anode-to-cathode spacings), the transient concentration of free cyanide can become significant and promote the oxidation and dissolution of a gold anode. High-current-density baths, especially those with high gold cyanide concentrations, are susceptible to the formation and buildup of Au(III) as $[Au(CN)_4]^-$ [17]. The presence of $[Au(CN)_4]^-$ will result in a lower apparent current efficiency at the cathode because it requires 3 eq mol^{-1} to deposit Au from Au(III) as opposed to 1 eq mol^{-1} for Au(I). This is different from the acid gold plating case where hydrogen gas was the side product responsible for lowering the plating efficiency. This creates a process control problem. As the Au(III) concentration builds up in the bath, the plating time, or current (coulombs per square centimeters) will have to be increased to achieve the same deposit thickness. Figure 4.5 shows the current efficiency and percent Au(III) in the bath as a function of weight of gold plated or number of bath turnovers for three different anodes [17]. The cathodic current density was 230–300 mA cm^{-2}, the anodic current density was 150–200 mA cm^{-2}, and the bath was the same as

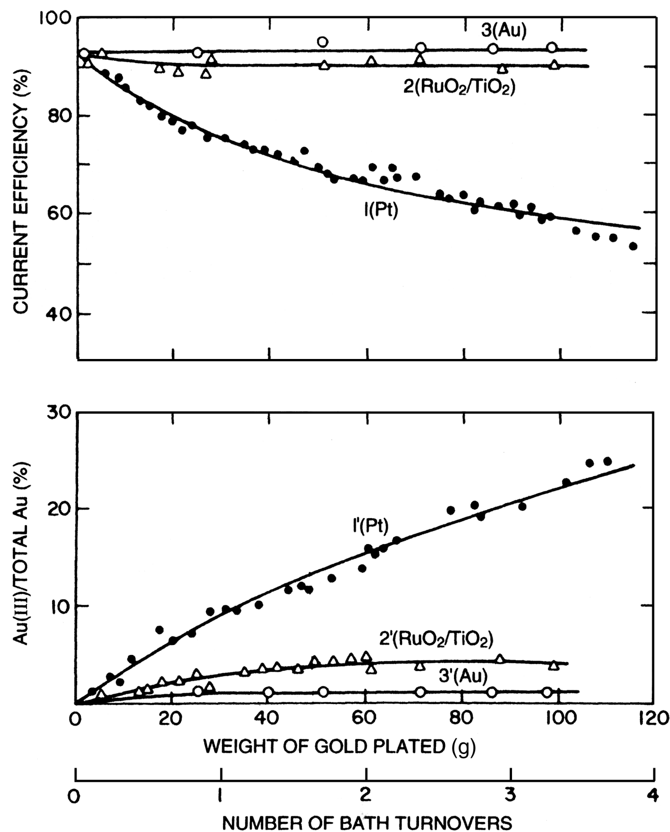

FIGURE 4.5 Variation in plating efficiency and Au(III) content with bath age (AFHG bath). (Curves 1, 1′: Pt anode; curves 2, 2′: RuO_2/TiO_2 anode, curves 3, 3′: Au anode.) (From Okinaka and Wolowodiuk [17].)

in Table 4.4 (high-speed bath). The gold anode did not result in a significant buildup of Au(III) because it was oxidized resulting in dissolution caused by the high transient concentration of free cyanide. The use of a gold anode is usually an unacceptable solution to the Au(III) problem because of the anode maintenance and changing cathodic current distribution as the anode corrodes and changes shape. The buildup of Au(III) is somewhat mitigated by the dilution effects due to drag-out. Other possible solutions to the Au(III) problem are to use a RuO_2/TiO_2 (often called dimensionally stable anode, DSA), adjust the current density to correct for the lower current efficiency, or chemically treat the Au(III) by reduction (e.g., hydrazine) or removal (activated carbon) [17].

4.1.4 Noncyanide Baths

The Au(I) cyanide complex is by far the most important for electrodeposition. However, there are several shortcomings to the use of $[Au(CN)_2]^-$ which have stimulated the investigation and commercialization of other gold complexes in plating baths [39]. The stability of the gold cyanide complex causes the reduction potential to occur at very negative potentials, resulting in the coreduction of hydrogen ions,

which lowers the plating efficiency and makes the development of electroless plating baths difficult [40]. The release of free cyanide during the reduction of $[Au(CN)_2]^-$ can be incompatible with positive photoresists used in the microelectronics industry [41, 42]. It has also been found that the residual stress of the plated gold can be controlled in noncyanide baths [43, 44]. Low-stress deposits are of particular interest for X-ray lithography masks because they must be thin, flat, and made from high-atomic-number elements. Lastly, the health and safety of workers and the environmental impact of the wide-scale use of cyanide are a concern.

The operating parameters of commercial gold sulfite baths have been presented with special attention given to the effect of plating temperature and current density on residual stress in the deposited metal [43, 44]. For example, Figure 4.6 shows the stress change from compressive to tensile as the temperature or current is raised. Thallium was used as the stress-reducing agent at concentrations up to 80 ppm, a value that can be more easily maintained than the low-thallium-concentration baths [43]. Alkaline sulfite baths can also be used without the use of thallium, which itself is a health hazard [44].

Although Au(I) sulfite has been used in commercial baths, the complex is susceptible to disproportionation, forming Au(III) and metallic gold. This spontaneous decomposition of the bath has led commercial baths to use proprietary stabilizing additives. Gold (I) sulfite (pK_a 10^{10}) is particularly troublesome at $pH < 7$ where sulfite protonates, forming bisulfite [45–48]. Gold (I) thiosulfate has a stability constant (pK_a 10^{28}) which is between that of Au(I) sulfite and Au(I) cyanide (pK_a 10^{39}). The Au(I) thiosulfate complex is stable in weakly acidic solutions because of the low pK_a for thiosulfate.

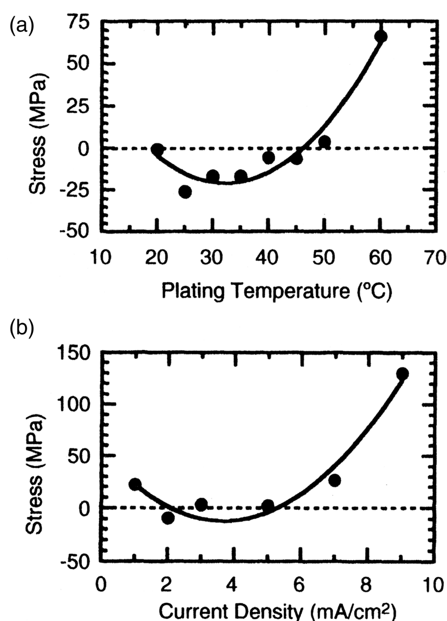

FIGURE 4.6 (*a*) Stress versus plating temperature for samples plated at 3 mA cm^{-2} form a bath containing 75 ppm thallium. (*b*) Stress versus current denisty for samples plated at 50°C from a bath containing 75 ppm thallium. (From Dauksher et al. [43].

The dominant species in mixed-complex baths, $S_2O_3^{2-}$ and $S_2O_3^{2-}$, at neutral or basic conditions have been reported to be $Au(S_2O_3)(SO_3)^{3-}$ [49]. The thiosulfate-only complex is dominant at low pH. The existence of the mixed ion complex was suggested in previous studies based on the deposition potential. It was also reported that the results from the sulfide-only bath are consistent with a higher stability constant (10^{27}), rather than the commonly assumed value of 10^{10} [49].

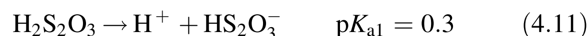

$$H_2S_2O_3 \rightarrow H^+ + HS_2O_3^- \qquad pK_{a1} = 0.3 \tag{4.11}$$

$$HS_2O_3^- \rightarrow H^+ + S_2O_3^{2-} \qquad pK_{a2} = 1.7 \tag{4.12}$$

The reduction of Au(I) thiosulfate was shown to have an overall reaction producing thiosulfate and gold [50]:

$$[Au(S_2O_3)_2]^{3-} + e^- \rightarrow Au + 2S_2O_3^{2-} \tag{4.13}$$

The standard heterogeneous rate constant for the reduction was found to be 1.6×10^{-3} cm s^{-1}, a transfer coefficient α of 0.23, and a diffusion coefficient of 7×10^{-6} cm^2 s^{-1} [40]. The effect of mixed thiosulfate–sulfite electrolytes has been studied shown to produce soft gold deposits suitable for forming gold "bumps" on ICs and in electronic interconnections [41]. The Vickers hardness of the electrodeposited gold was 80 kg mm^{-2} in the as-deposited state and 50 kg mm^{-2} after annealing. The optimum bath with thallium was composed of the following formulation:

$NaAuCl_4 \cdot 2H_2O$	0.06 *M*
Na_2SO_3	0.42 *M*
$Na_2S_2O_3 \cdot 5H_2O$	0.42 *M*
Na_2HPO_4	0.03 *M*
Tl^+ (added as Tl_2SO_4)	0.03 *M*
pH	6
Temperature	60°C
Current density	5 mA cm^{-2}

The mixed sulfide–thiosulfate plating bath was used to produce soft gold deposits for gold bumps and wire-bonding applications [51]. Bright gold deposits were obtained at a cathodic deposition efficiency (current efficiency) of greater than 99%. The purity of the gold deposits was greater than 99.99% and had a hardness between 60 and 80 Knoop. The bath composition is as follows:

Gold as metal	10 g L^{-1}
Sulfide	70 g L^{-1}
Thiosulfate	70 g L^{-1}
Additives	10 g L^{-1}
pH	5
Temperature	50°C

The deposition of gold from the iodide–thiosulfate bath was also studied [42]. It was suggested that the chemical reaction preceding the electron transfer step is the dissociation of the $[Au(S_2O_3)_2]^{3-}$ to form $[Au(S_2O_3)_2]^-$ and $S_2O_3^{2-}$

In each of the studies involving a mixed-thiosulfate bath (sulfite–thiosulfate and iodide–thiosulfate), it was observed that the mixed-salt gold complex is more stable and harder to reduce than either of the single-salt complexes [39–42]. That is, the Au(I) sulfite–thiosulfate complex is reduced at potentials more negative than either the Au(I) sulfite or Au(I) thiosulfate complex.

4.1.5 Gold Alloy Plating

The deposition of specific gold alloys has become important for specific industrial applications. Gold–tin alloys are useful as solders for electronic and optoelectronic die attachment. A weakly acidic, noncyanide electroplating solution based on gold and tin chloride salts with ammonium citrate as a buffer has been developed [52]. Tin contents from 27 to 42% were obtained:

Ammonium citrate	$200\,g\,L^{-1}$
$KAuCl_4$	$20\,g\,L^{-1}$
$SnCl_2 * 2H_2O$	$14\,g\,L^{-1}$
L-ascorbic acid	$30\,g\,L^{-1}$
$NiCl_2$	$1\,g\,L^{-1}$
Peptone	$5\,g\,L^{-1}$

Pulse plating was used with a similar chloride bath to produce alloys with a gold composition from 50 to 85% [53, 54]. It was shown that the microstructure produced under the pulsed-current conditions depended on the current density. At low current the grain growth occurred while at high current grain initiation was favored [55]:

Ammonium citrate	Buffer
$KAuCL_4$	$5\,g\,L^{-1}$
$SnCl_2 * 2H_2O$	$2–5\,g\,L^{-1}$
L-ascorbic acid	Tin stablizer
Ethylenediamine	$0.01–0.135$ moles L^{-1}
Sodium sulfite	Gold stablizer

A more traditional bath using $Au(CN)_2^-$ was used to obtain Au–Sn deposits [56]. The eutectic alloy is 71% atomic (or 80% by weight) gold. Alloys ranging from 75 to 98% gold were obtained by changing the bath composition and current density.

A variety of other gold alloys include gold–cobalt alloys deposited from a cyanide bath with an oxalate–citrate buffer and organic additives [57]. Gold–palladium alloys were deposited from an ionic liquid in the Lewis base form [58], and gold–silver was deposited from a cyanide bath by use of pulse plating [59].

4.2 MECHANISM OF DEPOSITION

Electrodeposition from the $[Au(CN)_2]^-$ complex is by far the most common and well studied. Two distinct mechanisms for gold deposition have been proposed [60–62]. The cathodic deposition of gold under activation control can be described by Butler–Volmer kinetics. At lower currents or less negative potentials the first step is the chemical adsorption of the $[Au(CN)_2]^-$ complex

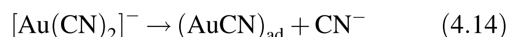

$$[Au(CN)_2]^- \rightarrow (AuCN)_{ad} + CN^- \qquad (4.14)$$

The electron transfer step is the rate-limiting one:

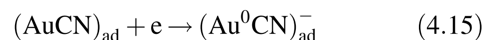

$$(AuCN)_{ad} + e \rightarrow (Au^0CN)^-_{ad} \qquad (4.15)$$

$$(Au^0CN)^-_{ad} \Leftrightarrow Au_{lattice} + CN^- \qquad (4.16)$$

The chemical desorption and crystallization make up the final step, as shown in Eq. (4.16) [61, 62]. The equilibria depend on the crystal orientation of the substrate and presence of impurities such as nickel or cobalt that can affect the nucleation rate and hardness of the gold. The Tafel slope at pH 4.4 for additive-free soft gold and nickel-hardened gold were found to be -0.35 and $-0.47\,V\,decade^{-1}$ respectively, as determined by chronopotentiometry and chronoamperometry [60]. The Tafel slope found for soft gold by linear sweep voltammetry was slightly smaller, $-0.39\,V\,decade^{-1}$. The smaller Tafel slope for nickel-hardened gold shows the strong inhibiting influence of nickel ions on the deposition process. It was found that at low current density ($0.25\,mA\,cm^{-2}$) a hexagonal crystalline structure was observed. The hexagonal structure dominates the deposit at short deposition times and is stabilized by metal ions in the bath, which led to underpotential deposition, such as Cu^{2+} and Tl^+ [63].

At more negative potentials, a second Tafel slope was obtained indicating a different mechanism for deposition, where the direct electroreduction of the gold cyanide ion takes place. Steeper Tafel slopes (more negative slopes) at higher currents were observed for soft gold ($-0.154\,V\,decade^{-1}$) and nickel-hardened gold ($-0.186\,V\,decade^{-1}$), as measured by chronopotentiometry and chronoamperometry. The two Tafel slopes were not observed by linear sweep voltammetry because nucleation begins gradually at less negative potentials and then the rate of crystal growth and nucleation increases, whereas the rates of nucleation and crystal growth are initially high for constant-potential or constant-current methods.

Surface-enhanced Raman spectroscopy (SERS) was used to examine the chemical moieties on the gold surface during deposition as a function of potential [64]. At high cathodic potentials and high current density ($1\,mA\,cm^{-2}$) the direct reduction of gold cyanide dominates. A SERS peak corre-

sponding to CN^- stretching of the absorbed species is observed. At more positive potentials and lower current density, (100 μA cm^{-2}), the mechanism shown in Eqs. (4.14), (4.15) and (4.16) dominates. The SERS peak broadening is consistent with this model. Similar methods were used to analyze the intermediates from deposition from $Au(CN^-)_4$ [65]. The results suggest that Au(III) also undergoes reduction via two different intermediates. The transition between the two mechanisms occurred at about the same potential for both Au(I) and Au(III). SERS was also used to show that the amount of hydrogen incorporation in the deposited gold could be reduced by using benzyldimethylphenylammonium chloride [66]. A peak at −0.7 V versus Ag/AgCl was linked to the conversion of the cyano group of the cyano-aurate complex into dyanide bonded to the metallic gold surface. A second peak at −1.05 V versus Ag/AgCl has been associated with the Au^0–CN to Au^0–NC reorientation.

In weakly acidic oxalate–phosphate baths, two Tafel regions were also found (−0.315 and −0.110 V $decade^{-1}$) for soft gold. Only one Tafel region was reported for hard gold (−0.200 V $decade^{-1}$); however, the nickel concentration was two orders of magnitude lower than that used in [60]. The linear sweep voltammograms show a strange dependence on the mass transport rate of the solution. In addition to the expected supply of reactants to the electrode surface, CN^- or HCN produced at the electrode surface can inhibit the reactions. Higher mass transport rates will reduce the concentration of these inhibitors at the surface.

The structure of electrodeposited soft gold is referred to as columnar because etched cross sections show long crystallites whose length axis coincides with the growth direction of the deposit. The nucleation rate of soft gold is low, and the tendency toward preferred growth on existing grains is high. In contrast, hard gold deposits have a high nucleation rate and submicrometer grain size, as noted earlier. Thus the principal difference between hard and soft gold is the grain size, which is derived from the rates of nucleation. That is, the effect of both impurities, current density, and other plating parameters on the mechanical properties of the deposit can be understood in terms of the nucleation and growth rate.

The surface roughness of gold deposits from a commercial gold cyanide solution was examined by scanning tunneling microscopy using smooth (111) gold surfaces [67]. It was found that the surface of the gold was roughened by simple immersion into the plating bath, an effect of the exchange current (the zero-applied-current) condition. The result of 100 Å of electrodeposited gold was “rolling hills” of gold 200 Å wide and 30 Å high.

4.3 PULSE PLATING

Pulse plating usually yields finer grain deposits than dc baths because of the high pulse current density and resulting high nucleation rate. Low porosity has been observed with pulse-plated gold due to grain refinement [68]. The growth of gold on crystalline copper is initially dependent on the structure of the substrate under pulse or dc plating. When the deposit reaches 50–100 nm in thickness, the growth gradually changes from substrate controlled to transport controlled [69]. In studies on orientated copper substrates, single-crystal growth was observed for [001] and [011] gold grains. The nuclei forming these grains coalesce when they come in contact with each other, which leads to single-crystal grain growth. For larger nuclei, the growing grains obtain equal orientation. These observations for pulse-plated gold are probably due to desorption of impurities during the relaxation time between successive pulses. Coalescence is more likely to occur if the growing surfaces are clean; if not, impurities are pushed into the film from the growing surface and prevent adjacent grains from coalescing, resulting in the formation of a grain boundary. Although the nucleation rate is high in pulse plating, the grain refinement is due to the different surface diffusion conditions. During pulse plating, the diffusion paths are blocked due to a high adion concentration, resulting in decreased surface mobility, and the structure becomes columnar. In dc plating, the adion mobility is high and a crystalline structure is developed [69]. The ductility, tensile strength, and yield strength were found to be improved in alternating current electrolysis; however, higher contact resistance was also reported [68]. The current distribution for selective pulse plating was quantitatively described as a function of peak current and anode-to-cathode ratio [70]. The current distribution is generally less uniform at small Wagner numbers. One problem common to all pulse plating strategies is the availability and cost of power supplies. The formation of high current pulses is expensive, and the rarity of users limits the benefits of mass production.

4.4 SUBSTRATE PREPARATION

Gold plating is often the last step in a long series of processing steps, making it immediately suspect when difficulties are encountered. However, in many cases the problems that appear at the gold plating step are due to the cleaning and preparation processes preceding gold deposition. Poor, incomplete, or inappropriate cleaning can result in inadequate gold deposits. While problems do occur in the gold plating process, only a good engineering evaluation of the defective deposits can elucidate the failure mechanism.

4.4.1 Cleaning and Surface Preparation

Copper, brass, and silver parts are easily plated once cleaned. The normal practice may require degreasing in an alkaline spray or soak or by a solvent vapor degreaser. A copper part may require a bright dip (10% sulfuric acid in water) to

remove the native oxide. Beryllium copper spring material or castings should be carefully cleaned by a 15-min soak in boiling NaCN and NaOH solution (38 g NaCN, 38 g NaOH, and 1 L H_2O) followed by a water rinse and bright dip and final rinse. Other procedures use a dip in 60% by volume H_2SO_4 at 50°C for 30 s followed by a water rinse.

Nickel parts must be activated before gold plating or the plate may peel. Activation can be accomplished by a dip in warm 1 : 1 HCl in water. It is very important not to allow the nickel parts to dry after activation before gold plating. Nickel alloys like Kovar can be cleaned by soaking for many minutes in hot 18% HCl. The oxide-free surface is prepared for plating by bright dipping for several seconds in 1 : 3 nitric acid–acetic acid with 15 mL HCl per liter of solution at 70°C. Kovar can be first plated with Woods or Watts nickel before gold plating or to gold strike the nickel alloy directly at high current in a low-gold-content bath followed by normal gold plating.

Gold plating onto aluminum and aluminum alloys has become more common, particularly for electronics and space applications. The surface is first degreased, such as in trichloroethylene vapors, followed by alkaline cleaning in trisodium orthophosphate (Na_3PO_4, 12 g L^{-1}; H_2O, 25 g L^{-1}; and Na_2CO_3, 20 g L^{-1}) at 60°C for 2–3 min. After water rinsing, the aluminum surface is cleaned in a mixed-acid solution (sulfuric acid, 10 mL L^{-1}; hydrofluoric acid (40%), 12.5 mL L^{-1}, and nitric acid, 25 mL L^{-1}) for 2–3 min. A zinc displacement deposition process can precede the electroless nickel underlayer (nickel sulfate, 30 g L^{-1}; zinc sulfate, 40 g L^{-1}; sodium hydroxide, 106 g L^{-1}; potassium cyanide, 10 g L^{-1}; potassium bitartrate, 40 g L^{-1}; copper sulfate, 5 g L^{-1}; and ferric chloride, 2 g L^{-1}) for 1 min. The first zinc layer is stripped in 50% nitric acid followed by a second zinc layer by immersion for 30 s [71]. Extreme caution should be practiced when handling hydrofluoric acid and potassium cyanide, especially when the cyanide is in the same vicinity as acids.

Gold films are widely used in MEMS applications because of its excellent physicochemical stability, low resistivity, and high reflectivity for infrared radiation. However, adhesion onto silicon has been problematic. A two-step electrodeposition process was found to give growth directly onto a silicon surface [72]. After stripping the surface oxide from the silicon, gold is plated and annealed and then a final coating of gold is plated. The current density of the initial gold plate is critical.

The adhesion of gold directly to glass is very difficult. An ion beam mixing process has been used to produce gold films directly bonded to glass [73]. An Au–C bilayer film was deposited on glass followed by ion beam "mixing" caused by the Xe^+ ion implantation. The ion implantation process provides for atomic mixing of the thin layer with the glass. A thicker film of gold could then be deposited. Excellent adhesion of the gold film on glass was obtained.

Thin electroplated gold wires were bonded to hydrogen silsesquioxane glass by a transfer process using imprint lithography [74]. The transfer process first produced thin gold wires on silicon from $AuCN_4^-$ immersion plating onto silicon. Silicon serves as the reducing agent for gold deposition. The plating bath contained free fluoride to dissolve the oxidized silicon. The lack of adhesion of the gold wire onto the silicon surface allows easy release and transfer onto the glass.

The direct thermocompression bonding of plated gold surfaces was used to achieve MEMS packaging [75]. Two silicon wafers were bonded together at a pressure of 2.5 MPa and temperature of 320°C. The gold film produced on the side walls of via holes was used for bonding to two parts together, providing a hermetic seal for the MEMS package.

4.4.2 Barrier Metals

Service requirements may need an underplate between the base metal and the gold electroplate. Specifications for gold-plated copper parts exposed to temperatures $> 60°C$ often require an intervening nickel-plated barrier to prevent copper–gold interdiffusion and subsequent copper bleed through to the surface. The barrier may be 5–10 μm of low-stress nickel, like that plated from a sulfamate bath. Gold plating on zinc-based alloys should have at least 8 μm of nickel over 8 μm of copper. Tin or lead should have 8 μm of nickel over 2 μm of copper.

4.4.3 Gold Strike

The use of a gold strike is common before the deposition of a thick gold plate. The thickness of a gold strike may be 0.02–0.25 μm, depending on the thickness and requirements of the full gold thickness. A gold strike bath is usually a dilute version of a normal gold plating bath. A high current density is used to overcome activation control of the plating process. A large fraction of the gold cyanide ions at the electrode surface are reduced to gold at a high nucleation rate. Thus a uniform deposit is formed over the electrode surface compensating for inhomogeneities across it, which may have created problems under normal gold plating conditions. The gold strike surface has increased adhesion and porosity, and less contamination is dragged into the main plating bath. A typical strike bath would have 0.8 g L^{-1} gold versus 8 g L^{-1} and current densities 2–10 times higher than the conventional bath.

4.4.4 High-Speed Strip Plating

There has been extensive use of high-speed plating as well as selective plating in the semiconductor industry since around 1970. In particular, reducing cost and materials in the reel-to-reel electroplating of electrical connectors has led to many

innovations in high-speed plating. Reel-to-reel plating of connectors includes facilities for cleaning and preparation of parts, strike plating, and transport of parts and chemicals. The sequence of the processes is similar to those in batch plating; however, size, space, and time limitations have stimulated a fine tuning of the processes, which makes their review worthwhile. The strip plating process for electrical connectors is composed of the following processes: (1) ultrasonic clean, (2) electropolish, (3) acid dip, (4) nickel plate, (5) gold strike, (6) hard gold plate, (7) hot rinse, and (8) dry [76]. Cleaning is limited to nonfoaming solutions because of the need for rapid recirculation of the liquid from a reservoir tank. Ultrasonic agitation speeds up the cleaning process by dislodging the contaminants from the surface through cavitation. Electropolishing is an anodic process where metal dissolves (cleaning and deburring) in proportion to the anode current density. Copper alloys used for electrical connectors electropolish well in 1 : 1 phosphoric acid in water. Current densities as high as $4000\,mA\,cm^{-2}$ can be used to accommodate high-speed processing with small electroplating cells. A major problem in electropolishing is the deposition of copper powder at the cathode, which must be removed periodically to avoid cell shorting. While it is desirable to have the electrodes in close proximity to reduce solution heating and voltage, wider spacing (e.g., 1.5 cm) is necessary to mitigate cell shorting from powdery copper loosely adherent to the cathode. The copper phosphate residue can be removed by a hot-water rinse followed by a rinse in 10% sulfuric acid (by volume) at 60°C. The nickel underplate ($\sim$0.14 μm) can be from a nickel sulfate or nickel sulfamate bath. The AFHG baths used in reel-to-reel gold strike are shown below:

	Gold Strike	High-Speed Bath
$KAu(CN)_2$	$4\,g\,L^{-1}$	$44\,g\,L^{-1}$
K_2HPO_4	$120\,g\,L^{-1}$	—
KH_2PO_4	$30\,g\,L^{-1}$	$100\,g\,L^{-1}$
KOH	—	$28\,g\,L^{-1}$
Temperature	65°C	40°C
pH	7.0	7.0

The current density for the gold strike is $30\,mA\,cm^{-2}$. The hardness of the final deposit is achieved by producing small grains, which is the result of high current density at low temperature. The hardness of the gold plated from the high-speed bath given above is 180 KHN_{25} for current densities between 150 and $250\,mA\,cm^{-2}$. The hardness drops off at lower current densities, to 150 KHN_{25} for $100\,mA\,cm^{-2}$, and 125 KHN_{25} at $50\,mA\,cm^{-2}$ [76]. Others have used even higher current densities (800–$2000\,mA\,cm^{-2}$), although the conditions are different [77]. A final hot rinse and drying complete the strip plating process. The plating process can be accomplished in relatively short-length plating cells ($\sim$18 in. long) with insoluble anodes that allow precise placement of the hardware in an attempt to selectively plate the gold only on the functional area of the connectors. Although a majority of the gold can be deposited on the contact area of connectors, it is extremely difficult to prevent some plating on nonfunctional areas immersed in the plating bath. Laser-assisted plating has been shown to assist in the selective plating process. Laser processes have been developed to improve the selectivity of the deposition process. The direct irradiation by a pulsed laser has been shown to cause extremely rapid surface heating, increasing the agitation and deposition rate. It also increases the interdiffusion of the deposited atoms [78, 79]. Lasers have also been used in a patterning technique where the whole component was coated with an insulator, such as glycol phthalate, paraffin wax, or photoresist, and an yttrium–aluminum–garnet (YAG) laser was used to burn off the material in small areas which were then plated [79]. One problem is the precise alignment of the laser to the part either in a moving or a step-and-repeat process.

4.5 STAINS

Staining of precious metal–plated surfaces is a critical concern, especially since chlorofluorocarbon (CFC) usage is discouraged. The CFC displacement method did not dry the plated metal surface; it displaced the water from the plated surface. The plating stains are often caused by potassium cyanide or other plating salts precipitating on the surface as the water evaporates. Stains are often seen as irregularly shaped "hollow" blemishes where the stained area is smaller than the original water drop size, and the center of the stain is not very discolored. Droplets form on the wetted areas as the plated parts are removed from the rinse water. The rinsing water simply dilutes the plating salts, leaving a low concentration of salt. As the rinse water dries from the surface, the volume of the original water droplet is reduced through evaporation. The concentration of the salt in the droplet increases as the volume decreases. When the concentration of the salts exceeds their solubility, they precipitate onto the surface. The "hollow" center is formed because the salts continue to precipitate onto the existing deposit. The oxidation of the gold surface is not an issue as it would be with less noble metals. There are many things which can be done to reduce the staining of electroplated gold parts: (1) use high-quality rinse water, (2) countercurrent rinsing techniques are desirable, (3) removing the final rinse water from the surface by CFC displacement, and (4) removal of rinse water by hot air knives, centrifugal dryers, or alcohol absorption. Isopropyl alcohol is often preferred, especially over methanol because the rate of evaporation is slower. Rapid evaporation can result in cooling of the surface below the ambient dew point, resulting in condensation of water and nucleation of spots.

4.6 TEST METHODS

The physical properties of significance for the gold deposits are appearance, wear resistance, hardness, brittleness, residual stress, porosity, thickness, density, and deposit uniformity. The chemical properties of importance include the chemical composition of the deposits and solutions, segregation of impurities, and inertness to oxidation. Each of the physical and chemical properties can be tested.

4.6.1 Physical Properties

Appearance tests are often subjective and reflect only the surface texture and color of the deposit. Color match and uniformity are critical for decorative plating. The appearance is best controlled through strict control of the plating variables. Changes in the deposit are often the result of unintentional codeposition of unwanted metals. Lead from solder baths and iron from plating fixtures are common problems. Burned deposits can be the result of a depleted bath, excessively high current density, or non uniform current distribution such as would occur from defective or misshaped anodes.

Wear resistance is an important attribute for gold finishes in high-wear situations, such as sliding contacts. An abrasive test applicable to jewelry applications has been described [80]. Wear tests applicable to electrical parts have been described [24, 25, 80, 81]. The purpose of the tests is to determine how fast a deposit fails under laboratory-imposed mechanical loads, with commercial testers providing a convenient method for comparison. The variables include shape of the parts exposed to wear, cleaning, lubrication, and load.

Deposit hardness can be determined by mechanical deformation of test specimens. Commercial instrumentation and scales of hardness exist [82]. Two of the most common instruments use pyramidal diamond indenters with equal (Vickers) or unequal (Knoop) diagonals. The use of these for gold parts has been discussed [83]. Hardness is usually determined using cross sections of suitable thickness. Indenting normal to the surface often leads to erroneous results because surface roughness can lead to nonuniform loads and thin samples give hardness representative of the base substrate and not the plated gold. Electroplated soft gold has a Knoop hardness of about 60 under a 25-g load. Hard gold can have Knoop values near 200.

Brittleness is the result of the presence of some particular phase or compound in the gold, such as can occur by the alloying of gold, either intentional or unintentional. Nickel and cobalt are intentionally added to improve hardness, whereas tin can cause brittle solder joints [84]. When all the gold does not dissolve in the solder, brittle failure can occur. Identification of brittle failures can be performed through metallographic examination. Gold hardened by codepositon of iron at the 0.1% level leads to stressed deposits that are brittle and that fail under mechanical loads milder than acceptable for printed wiring boards and connectors. Iron contamination is a particular concern because of the ease of contamination of gold baths from steel components. The degree of brittleness can be quantified in a flex test of the deposit, such as bending mandrill tests. Other tests include uniaxial tensile tests and diamond scribe tests [32].

Pure gold is electrodeposited in virtually a zero-stress state. The gold can be brought to a low-stress state if it is deposited onto a substrate whose coefficient of thermal expansion is different from gold and the deposition occurs at other than room temperature. During cooling from the deposition temperature, the different rate of contraction of the gold and its substrate produces residual stress. Temperature cycling of plated gold onto a substrate can result in significant stress, depending on the temperature excursion. At sufficiently high temperatures ($\sim$150°C), gold can recrystallize, reducing the stress at high temperature via grain growth. Upon cooling, the process is not reversible. That is, the coefficient of thermal expansion mismatch will produce a high-stress state in the gold.

There are several common test methods for porosity [85]. Chemical tests are used to determine the area of the exposed base metal by visual examination of the quantity of accumulated corrosion products. The base metal is oxidized by anodic dissolution or by chemical attack. This class of tests are easy to perform. Common forms of the test use polysulfide solutions [86] or atmospheres containing moist sulfur dioxide [87, 88] or nitric acid [85, 89]. The electrooxidation of the gold-plated part using a moist paper or a gel as a support for the electrolyte containing a dye or complexing agent can be used to quantify the porosity of the gold [90]. In the test, the complexed gold forms a colored species that can easily be identified and counted. Specific tests have been developed for copper and nickel.

The electromigration resistance of gold was measured using a four-terminal Kelvin line structure using a stress current of 2.0 MA cm^{-2} at temperatures between 325 and 375°C [91]. The activation energy for electromigration was 0.59 ± 0.09 eV. A diffusion mechanism for void formation was suggested. The Young's modulus, residual stress, and stress gradient in electroplated films were measured using surface micromachined beam structures [92]. The Young's modulus was calculated to be from 35.2 to 43.9 GPa using a value of Poisson's ratio of 0.42 for gold.

4.6.2 Chemical Analysis

Atomic absorption (AA) spectrophotometry is a rapid and easy method for analyzing gold films. The gold deposit can be separated from the base metal by immersing the part in an etchant that oxidizes and dissolves the base metal without oxidizing the gold or leaching out its impurities. The gold is then dissolved and the solution is analyzed by AA using the

appropriate standards. Such tests are needed in meeting specifications such as military specification MIL-G-45204B for pure, bondable gold where metallic impurities such as chromium, copper, tin, lead, silver, cadmium, or zinc should not be present in the deposit at a concentration greater than 0.1 %. Polarography can be used to analyzed solutions for various impurities and well as the gold baths themselves. The concentration of Au(III) has been quantified by polarography [17]. More exotic techniques can be used for specific analysis. For example, Mossbauer spectroscopy of Fe^{57} was used to uncover the form of the cobalt in gold deposits [22]. Radioactive Co^{57} was added to the common Co^{59} additive in the cobalt-hardened bath. The Co^{57} decayed to Fe^{57}, which could be studied by Mossbauer spectroscopy. Another example of a specific analytical method is the analysis of carbon. The carbon content of the deposits has been determined by combustion, converting it to CO_2, which could be measured by coulometric titration [93].

Surface analytical techniques, such as Auger electron spectroscopy and X-ray photoelectron spectroscopy, are often used to determine the elemental analysis of the gold surface as well as thin surface films when combined with sputter etching. Rutherford backscattering (α-particle backscattering) is a powerful technique for identifying impurities and the distribution of impurities with depth in a rapid and nondestructive test. The thickness of thin films of gold can also be determined [94]. β-ray scattering can also be used for thickness measurements, and the apparatus is quite simple. X-ray fluorescence can also be used for thickness and impurity analysis; however, standards and tight control of analysis geometry are essential for accurate results. Structural aspects of gold deposits, such as grain size, are best determined by transmission electron microscopy. While sample preparation can require considerable effort, the results are irreplaceable [34, 43]. A technique known as through-focus imaging was used to observe organic and gaseous inclusions in gold, which cannot be done by conventional imaging techniques [34]. The availability of scanning probe techniques has provided new tools for examining growth and nucleation of deposits [67]. Last, surface contamination of electrical parts has created a need for evaluating and monitoring the contact resistance of electrical parts. Typical values of about 1 mΩ are obtained for electrical contacts. The contact force and area of the contact need to be controlled. Contact resistance increases of 2- to 50-fold have been observed for aged cobalt-hardened gold [32].

REFERENCES

1. G. Langbein and W. T. Brannt, *Electroplating of Metal*, 4th ed., Henry Carey Baird and Co., Philadelphia, PA, 1902, p. 3.
2. M. Pourbaix, *Atlas of Electrochemical Equilibra in Aqueous Solutions*, Pergamon, New York, 1966.
3. W. M. Latimer, *The Oxidation States of the Elements and Their Properties in Aqueous Solutions*, Prentice-Hall, Englewood Cliffs, NJ, 1985.
4. G. M. Schmid and M. E. Curly-Florino, in *Encyclopedia of Electrochemistry of the Element*, Vol. 4, A. J. Bard, Ed., Marcel Dekker, New York, 1978.
5. R. Puddephatt,in *Comprehensive Inorganic Chemistry*, Vol. 4, J. C. Bailar Jr., H. J. Emeleus, R. Nyholm, and A. F. Trotman-Dickenson, Eds., Pergamon, Elmsford, NY, 1973.
6. G. H. Kelsall, *J. Electrochem. Soc.*, **138**, 108 (1991).
7. W. T. Lee, *Corrosion Technol.*, **39** (Apr. 1963).
8. E. D. Winters, *Plating*, **59**, 213 (1972).
9. S. A. Losi, F. L. Zuntini, and A. R. Meyer, *Electrodeposition Surf. Treatment*, **1**, 3 (1972).
10. L. Silverman, B. Bernauer, and F. Pettinger, *Met. Finish.*, **68**, 48 (Aug. 1970).
11. W. A. Fairweather, *Met. Finish.*, **64**, 15 (May 1986).
12. J. M. Leeds and M. Clarke, *Trans. Inst. Met. Finish.*, **47**, 163 (1969).
13. H. Angerer and N. Ibl, *J. Appl. Electrochem.*, **9**, 219 (1979).
14. Y. Okinaka, F. B. Koch, C. Wolowodiuk, and D. R. Blessington, *J. Electrochem. Soc.*, **125**, 1745 (1978).
15. E. D. Winters, *Plating*, **59**, 213 (1972).
16. Y. Okinaka and S. Nakahara, *J. Electrochem. Soc.*, **123**, 1284 (1976).
17. Y. Okinaka and C. Wolowodiuk, *J. Electrochem. Soc.*, **128**, 288 (1981).
18. A. Knodler, *Metalloberflache*, **28**, 465 (1974).
19. C. J. Raub, A. Knodler, and J. Lendvay, *Plating*, **63**, 35 (1976).
20. Y. Okinaka, F. B. Koch, C. Wolowodiuk, and D. R. Blessington, *J. Electrochem. Soc.*, **125**, 1745 (1978).
21. H. Leideiser, Jr., A. Vertes, M. L. Varsanyi, and I. Czako-Nagy, *J. Electrochem. Soc.*, **126**, 391 (1979).
22. R. L. Cohen, F. B. Koch, L. N. Schoenberg, and K. W. West, *J. Electrochem. Soc.*, **126**, 1608 (1979).
23. C. C. Lo, J. A. Angis, and M. R. Pinnel, *J. Appl Phys.*, **50**, 6887 (1979).
24. K. J. Whitlaw, J. W. Souter, I. S. Wright, and M. C. Nottingham, *IEEE Trans. CHMT*, **8**, 46 (1985).
25. L.-G. Liljestrand, L. Sjohren, L. B. Revay, and B. Asthner, *IEEE Trans. CHMT*, **8**, 123 (1985).
26. J. H. Thomas III and S. P. Sharma, *J. Electrochem. Soc.*, **126**, 445 (1979).
27. G. B. Munier, *Plating*, **56**, 1151 (1969).
28. L. Holt, R. J. Ellis, and J. Stanyer, *Plating*, **60**, 910 (1973).
29. M. Antler, *Plating*, **60**, 468 (1973).
30. H. A. Reinheimer, *J. Electrochem. Soc.*, **121**, 490 (1974).
31. R. L. Cohen, K. W. West, and M. Antler, *J. Electrochem. Soc.*, **124**, 342 (1977).
32. F. B. Koch, Y. Okinaka, C. Wolowodiuk, and D. R. Blessington, *Plating*, **67**, 50 (1980).
33. H. A. Reinheimer, *J. Electrochem, Soc.*, **121**, 490 (1974).
34. S. Nakahara and Y. Okinaka, *J. Electrochem. Soc.*, **128**, 284 (1981).

35. F. B. Koch, Y. Okinaka, C. Wolowodiuk, and D. R. Blessington, *Plating*, **67**, 43 (1980).
36. S. Kal, A. Bagolini, B. Margesin, and M. Zen, *Microelectron. J.*, **37**, 1329 (2006).
37. J. J. Kelly, N. Yang, T. Headley, and J. Hachman, *J. Electrochem. Soc.*, **150**, C445 (2003).
38. A. Chinthakindi, D. Bhusari, B. Dusch, J. Musolf, B. Willemsend, E. Prophet, M. Roberson, and P. A. Kohl, *J. Electrochem. Soc.*, **149**, HI39 (2002).
39. M. Paunovic and C. Sambucetti, in *Electrochemically Deposited Thin Films, Proc.*, Vol. 94–31, M. Paunovic, Ed., Electrochemical Society, Pennington, NJ, 1995, pp. 34–44.
40. A. M. Sullivan and P. A. Kohl, *J. Electrochem. Soc.*, **144**, 1686 (1997).
41. T. Osaka, A. Kodera, T. Misato, T. Homma, Y. Okinaka, and O. Yoshioka, *J. Electrochem. Soc.*, **144** (1997).
42. X. Wang, N. Issaev, and J. G. Osteryoung, *J. Electrochem. Soc.*, **144** (1997).
43. W. J. Dauksher, D. J. Resnick, W. A. Johnson, and A. W. Yanof, *Microelectron. Eng.*, **23**, 235 (1994).
44. W. Chu, M. L. Schattenburg, and H. I. Smith, *Microelectron. Eng.*, **17**, 223 (1992).
45. H. Homma and Y. Kagaya, *J. Electrochem. Soc.*, **140**, L135 (1993).
46. T. Inoue, S. Ando, H. Okudaira, J. Ushio, A. Tomizawa, H. Takehara, T. Shimazaki, H. Yamamoto, and H. Yokono,in *Proc. 45th Electronic Components and Technology Conf.*, IEEE, New York, 1995, p. 1059.
47. M. Kato, K. Nikura, S. Hoshino, and I. Ohono, *J. Surf. Finish. Soc. Jpn.*, **42**, 69 (1991).
48. Y. Okinaka and T. Osaka,in *Advances in Electrochemical Science and Engineering*, Vol. 3, H. Gerischer and C. Tobias, Eds., VCH Publishing, New York, 1994, p. 55.
49. T. A. Green and S. Roy, *J. Electrochem. Soc.*, **153**, C157 (2006).
50. A. M. Sullivan and P. A. Kohl, *J. Electrochem. Soc.*, **142**, 2250 (1995).
51. K. Wang, R. Beica, and N. Brown, *29th International Manufacturing Technology Symposium,* IEEE/SEMI, 2004, pp. 242– 246.
52. W. Sun and D. Ivey, *Mat. Sci. Eng.*, **B65**, 111 (1999).
53. J. Doesberg and D. Ivey, *Plating Surf. Finish*, **88**, 78 (Apr. 2001).
54. A. He, B. Djurfors, S. Aldhlaghi, and D. Ivey, *Plating Surf. Fin.*, **89**, 48 (Nov. 2002).
55. J. Doesberg and D. Ivey, *Mater. Sci. Eng.*, **B78**, 44 (2000).
56. G Hoimbom, J. Abys, H. Straschil, and M Svensson, *Plating Surf. Finish*, (Apr. 1998).
57. L. Chalumeau, M. Wery, H. Ayedi, M. Chabouni, and C. Leclere, *Surf. Coating Tech.*, **201**, 1363 (2006).
58. F. Su, J. Huang, and I. Sun, *J. Electrochem. Soc.*, **151**, C811 (2004).
59. H. Sanchez, P. Ozil, E. Chainet, B. Nguyen, and Y. Meas, *J. Electrochem. Soc.*, **144**, 2004 (1997).
60. W. Chirzanowski, Y. G. Li, and A. Lasia, *J. Appl. Electrochem.*, **26**, 385 (1996).
61. E. T. Eisenmann, *J. Electrochem. Soc.*, **125**, 717 (1978).
62. G. Holmbom and B. E. Jacobson, *J. Electrochem. Soc.*, **135**, 787 (1988).
63. B. Bozzini, G., Giovannelli, S. Natali, A. Fanigliulo, and P. Cavallotti, *J. Mater. Sci.*, **37**, 3903 (2002).
64. B. Bozzini, C. Mele, and V. Romanello, *J. Electroanal. Chem.*, **592**, 25 (2006).
65. B. Bozzini, B. Busson, G. De Gaudenzi, L. D'Urzo, C. Mele, and A. Tadjeddine, *J. Electroanal. Chem.*, **602**, 61 (2007).
66. A. Fanigliulo and B. Bozzini, *J. Electroanal. Chem.*, **530**, 53 (2002).
67. J. Schneir, V. Elings, and P. K. Hansma, *J. Electrochem. Soc.*, **135**, 2774 (1988).
68. G. Decaraj and S. Gurrviah, *Mater. Chem. Phys.*, **25**, 439 (1990).
69. G. Holmbom and B. E. Jacobson, *J. Electrochem. Soc.*, **135**, 2720 (1988).
70. D. T. Chin, N. R. K. Vilambi, and M. K. Sunkara, *Plating*, **76**, 74 (1989).
71. A. K. Sharma, *Trans. Inst. Met. Finish.*, **67**, 87 (Aug. 1989).
72. T. Fujita, S. Nakamichi, S. Iodu, K. Maenaka, and Y. Takayama, *Sensors Actuators A*, **135**, 50 (2007).
73. L. Guzman, A. Miotello, R. Checchetto, and M. Adami, *Surf. Coating Tech.*, **158**, 558 (2002).
74. J. Chen. J. Liu, Y Hsu, J. Syu, and S. Huang, *Nanotechnology*, **16**, 2913 (2005).
75. G. Park, Y. Kim, K. Paek, J. Kim, J. Lee, and B. Ju, *Electrochem. Solid-State Lett.*, **8**, G330 (2005).
76. D. R. Turner, *Met. Finish.*, **63**, 41 (Nov. 1987).
77. D. W. Endicott and G. J. Casey, Jr., *Plating*, **67**, 58 (1980).
78. R. J. von Gutfeld, M. H. Gelchins, and L. T. Romankiw, *J. Electrochem. Soc.*, **130**, 1840 (1983).
79. I. R. Christie, *Trans. Inst. Met. Finish.*, **64**, 47 (1986).
80. R. Duva and D. G. Foulke, *Plating*, **55**, 1056 (1968).
81. A. J. Solomon and M. Antler, *Plating*, **57**, 812 (1970).
82. V. E. Lysaght, *Indentation Hardness Testing*, Reingold, New York, 1948.
83. R. G. Baker and T. R. Palumbo, *Plating*, **58**, 791 (1971).
84. F. G. Foster, *ASTM Spec. Tech. Pub.*, **319**, 3113 (1963).
85. A. A. Khan, *Plating*, **56**, 1374 (1969).
86. F. I. Nobel, B. D. Ostrow, and D. W. Thomson, *Plating*, **52**, 1001 (1965).
87. R. W. Beattie, G. Forshow, and E. N. Loney, *Proc. IEE (London)*, **B-109** (suppl. 21), 109 (1962).
88. M. Clarke and J. M. Leeds, *Trans. Inst. Met. Finish.*, **46**, 81 (1968).
89. F. Knoop, C. G. Peters, and W. E. J. Emerson, *J. Res. Natl. Bur. Stand.*, **23**, RP 1220 (1939).
90. F. V. Bedette and R. V. Chiarinzelli, *Plating*, **53**, 305 (1956).
91. S. Kilgore, C. Gaw, H. Henry, D. Hill, and D. Schroder, *Mater. Res. Soc. Symp. Proc*, **863**, B8.30.1 (2005).
92. C. Baek, Y. Kim, Y. Ahn, and Y. Kim, *Sensors Actuators A*, **117**, 17 (2005).
93. E. N. Wiese, P. W. Gilles, and C. A. Reynolds, *Anal Chem.*, **25**, 1344 (1953).
94. J. Zahavi, *Met. Finish.*, **83**, 61 (July 1985).